Regulation Flexibility Assessment and Optimal Aggregation Strategy of Greenhouse Loads in Modern Agricultural Parks

Shiwei Xia, *Senior Member*, *IEEE*, Liuyang Cai, Mingze Tong, Ting Wu, Peng Li, and Xiang Gao

***Abstract*—With advances in modern agricultural parks, the rural energy structure has undergone profound change, leading to the emergence of an agricultural energy internet. This integrated system combines agricultural energy utilization, the information internet, and agricultural production. Accordingly, this study proposes a regulation flexibility assessment approach and optimal aggregation strategy of greenhouse loads (GHLs) for modern agricultural parks. First, taking into ac-count the operational characteristics of typical GHLs, refined load demand models for lighting, humidification, and temperature-controlled loads are established. Secondly, the recursive least squares method-based parameter identification method is designed to accurately determine key GHL model parameters. Finally, based on the regulation flexibility of quantitatively evaluated GHLs, GHLs are optimally aggregated into multiple flexible aggregators considering minimal operational cost and greenhouse environmental constraints. The results indicate that the proposed regulation flexibility assessment approach and optimal aggregation strategy of GHLs can alleviate the peak regulation pressure on power grids by flexibly shifting the load demands of GHLs.**

***Index Terms*—Agricultural park, greenhouse load; parameter identification, regulation flexibility, optimal aggregation of GHLs.**

I. Introduction

Rural power grids serve as crucial links connecting the supply and demand sides of rural energy, and play a significant role in the development of a low-carbon countryside [1]. The agricultural energy internet (AEI) integrates agricultural energy with the Internet and promotes agricultural electrification in the countryside [2]. It also provides real-time regulation of light, temperature, and humidity environments in agricultural parks via electrical facilities such as LED lighting, electric heating panels, pumps, and ventilators to achieve a deep coupling between agriculture and energy [3]–[5]. With the continuous development and extension of AEI, the electricity load in rural areas experiences continuous growth with noticeable peaks and valleys, presenting a significant challenge to power systems [6]. Hence, research is being under-taken to fully exploit the regulation potential of rural energy and integrate the operation of agricultural flexible loads with AEI [7].

However, current studies on the participation of flexible loads in grid dispatch are primarily focused on the analysis of the regulation potential of urban loads.

Reference [8] establishes a physical model of the equivalent thermal parameters of residential air conditioning loads, and evaluates the maximum regulation potential of aggregated air conditioning loads based on an improved discrete particle swarm algorithm. In [9], a constant current-voltage variable power model is introduced to describe the charging and discharging processes of electric vehicles and a regulation potential assessment method is proposed that accounts for the difference in dispatch and user-side demand. Reference [10] considers air conditioning loads and electric vehicles. These account for a relatively large share of residential electricity loads. It takes them as re-search objects and develops mathematical models in terms of user comfort and physical levels to fully exploit the regulation potential of flexible demand-side loads. In [11], the effectiveness of flexible loads in reducing peak-to-valley amplitude and volatility is verified by using the "source-load-storage" collaborative response distribution optimization method. In [12], a model is proposed for evaluating the regulation potential of electric vehicles based on the analysis of power constraints and the vehicles' available capacity. Reference [13] models air conditioning systems as virtual energy storage systems and analyzes the control mode and regulation strategy for the participation of air conditioning systems in demand response.

Similar to flexible loads in urban areas, agricultural loads are controllable. Reference [14] proposes a basic framework for the participation of agricultural loads in

Received: July 30, 2023
Accepted: December 10, 2023
Published Online: May 1, 2024
Ting Wu (corresponding author) is with the School of Mechanical Engineering and Automation, Harbin Institute of Technology, Shenzhen 518055, China (e-mail: twu920@hotmail.com).
DOI: 10.23919/PCMP.2023.000025

grid dispatch considering grid demand, response market mechanisms, and load characteristics, with several factors limiting the participation of agricultural loads in demand response mechanisms deemed as entry points. In [15], the impact of time-shifted characteristics of agricultural loads on the scale of investment in renewable energy systems is discussed based on a stochastic scenario planning model. [16] evaluates the regulation potential of agricultural loads in the power system by collecting historical data from Gujarat, India, using crop irrigation loads as an example. However, agricultural loads are significantly different from the urban load. This difference is mainly in the deep coupling between energy and agricultural production. Agricultural control loads such as LEDs, heaters, etc. change the agricultural environment by using energy for generating heat, light, and humidity, etc., and different types of environmental control loads will have varied impacts on the agricultural system [17]. Taking the example of the greenhouse in crop production, the temperature-controlled loads are affected by many factors, such as light intensity, crop types, crop growth period, etc., making their modeling more complex than urban loads [18]. Consequently, the uniqueness of agricultural loads makes the existing technology inapplicable. Therefore it is necessary to study the modeling and scheduling of agricultural load flexibility, and to fully explore their flexible regulation ability.

With the rapid development of agricultural modernization, many studies have been carried out on greenhouse modeling and energy consumption. In [19], a dynamic response model of plant growth and greenhouse temperature is established by using a non-linear autoregressive neural network, and the validity of the model is verified using a non-destructive continuous system based on weighing sensors in 60 days of greenhouse cultivation. [20] constructs an adaptive model of greenhouse ambient temperature based on parameter identification. It characterizes the nonlinear and time-varying correlation between natural ventilation and temperature, and realizes adaptive control of loads using the identification toolbox. From the characteristics of an agricultural greenhouse, [21] analyzes the time-lapse characteristics of agricultural loads, and establishes the electricity, heat and multi-energy scheduling model of microgrids for economic operation. [22] proposes a solar soil heat storage system for greenhouse heating, one which uses the solar energy stored in greenhouse soil to heat the greenhouse, so as to reduce the energy demand of temperature-controlled loads in extreme weather and alleviate the heat supply and demand imbalance in summer and winter. Reference [23] combines photovoltaic power generation with a tomato greenhouse cogeneration system. Through technical and economic analysis, it is found that the system can not only meet 73% of the heat demand of the greenhouse but also provide 2.6 times the net power output, which greatly improves energy efficiency.

From existing studies, although good accuracy has been achieved in the greenhouse model, two limitations still exist. First, the dynamic impact of agricultural loads on the greenhouse environment is not considered in the models, so they fail to reflect the flexibility characteristics. Secondly, current research on the modes and strategies for agricultural load participation in agricultural energy dispatch is relatively limited. Flexible loads are optimally regulated after single aggregation in typical long-time scale scenarios, aiming for optimal economic operational cost [24], maximum new energy consumption [25], highest customer satisfaction [26], etc. Conversely, for agricultural loads, because of a variety of loads and large variability in resource characteristics [27], the use of a global integration optimization method in-creases the complexity and solution time.

To address the above challenges, this study considers greenhouse loads (GHLs) in agricultural parks as the research object, establishes a refined model for various types of GHLs, and proposes a model parameter identification method based on a recursive least squares (RLS) strategy. By quantitatively calculating the regulation potential of each type, the GHLs are optimally aggregated into a certain number of aggregators in terms of the lowest regulation cost, and the configured aggregators are called in order of priority during intra-day operation to satisfy the grid side regulation demand.

The innovatory aspects of this study can be summarized as follows:

1) With agricultural energy endowment, the time-shift energy consumption characteristics of GHLs are analyzed, and the load demand models of lighting load (LL), humidification load (HL), and temperature-controlled load (TL) are established for regulation flexibility assessment.

2) An RLS strategy-based parameter identification method is designed to accurately determine key GHL model parameters, and parameter sensitivity analysis is also conducted to adjust the load control cycles of GHLs.

3) GHLs are optimally aggregated into multiple flexible aggregators while considering minimal operational cost and greenhouse environmental constraints, and the case study verifies the effectiveness of the proposed optimal GHL aggregation strategy.

The remainder of this paper is organized as follows. Section II presents the flexible characteristics of GHLs and establishes the load demand models. Section III proposes a parameter identification method based on RLS. Section IV proposes a calculation method for the regulation potential of GHLs and establishes the optimization aggregation model. Section V considers a modern agricultural park in December as an example to analyse the results. Section VI presents the main conclusions of the paper.

II. Characterization and Modeling of GHLs

A. Load Characteristics and Classification

GHLs can be classified into four categories according to their regulation characteristics relating to electrical energy [28]: 1) interruptible loads (IL), such as cleaning equipment, submersible pumps, and negative air pressure machines; 2) shiftable loads (SL), such as LEDs, and agricultural tram charging and discharging; 3) curtailable loads (CL), such as carbon crystal electric heating panels and panning water sprinklers; and 4) uncontrollable loads (UL), such as ventilation fans and monitoring systems.

The classification and characteristics of common GHLs are presented in Table I.

TABLE I
Characteristics of Each Load in the Greenhouse

Load type	Use	Use time	Category	Power (kW)	Load type	Use	Use time	Category	Power (kW)
Microwave sulfur lamp	Light supplementation	10 h per day	IL SL	3.4	Organic fertilizer dispenser	Fertilizer application	09:00–21:00	IL SL	2.7
Sound wave booster	Yield increase	06:00–20:00	IL SL	3.2	Nutrient sterilizer	Fungicide	09:00–21:00	IL SL	2.5
Negative air pressure machine	Ventilation	06:00–21:00	IL	3.5	Submersible pump	Water pumping	00:00–24:00	IL SL	3.9
Circulating ventilator	Ventilation	06:00–21:00	IL	2.9	Panning water sprinkler	Irrigation & Humidification	09:00–21:00	CL IL	3
Water & Fertilizer integration	Fertilization & Irrigation	09:00–21:00	IL	2	Carbon crystal electric heating panel	Heating up	00:00–24:00	CL IL	10
Electric shock insecticidal lamp	Insecticide	09:00–21:00	IL SL	2	Far infrared heating	Keeping warm	20:00–06:00	CL IL	6.7
Plasma nitrogen fixation	Fertilizer supplementation	09:00–21:00	IL SL	2.9	Space electric field	Purification & yield increase	00:00–24:00	IL SL	3
Fans coil	Cooling	00:00–24:00	CL IL	6.2	Agricultural tram	Transporting seeds	00:00–24:00	SL	35
LED lighting	Light supplementation	06:00–21:00	IL SL	3	Ventilation fan	Aeration	00:00–24:00	UL	3
Cleaning equipment	Cleaning	08:00–21:00	IL	4	Monitoring system	Control	00:00–24:00	UL	1.5

B. Load Modeling

1) Lighting Load Model

LL primarily provides crops with the necessary light intensity, which can be modeled as [29]:

$$P_{\text{light}}(t)=\frac{S_{\text{gh}}\phi_0 C_1 C_2}{\eta_{\text{light}}}I_{\text{e}}(t) \tag{1}$$

$$I_{\text{e}}(t)=\frac{I_{\text{set}}-\lambda I_{\text{out}}(t)}{k_{\text{light}}}\times 1000 \tag{2}$$

where $P_{\text{light}}(t)$ is the power of LL at time t; S_{gh} is the total area of the greenhouse; ϕ_0 is the luminous flux per unit area; C_1 and C_2 are correction coefficients; η_{light} is the electrical conversion efficiency of LL; $I_{\text{e}}(t)$ is the average illuminance at time t; which can be expressed using the unit capacity method [30]; I_{set} is the indoor set light intensity; λ is the light transmission rate of the greenhouse; $I_{\text{out}}(t)$ is the outdoor radiation flux at time t; and k_{light} is the illuminance conversion factor.

2) Humidification Load Model

Humidity is an extremely important influencing factor in the environment of greenhouses, and is primarily affected by three components: water vapor evaporated from the soil surface, water vapor lost from ventilation, and water vapor generated from HL. Therefore the following humidity balance model can be established:

$$\begin{aligned}H_{\text{pen}}(t)=s_{\text{pen}}(t)m_{\text{pen}}\alpha[e'(T_{\text{in}}(t))-e(T_{\text{in}}(t))]=\\ H_{\text{in}}(t)-H_{\text{soil}}(t)-H_{\text{air}}(t)\end{aligned} \tag{3}$$

where $H_{\text{pen}}(t)$ is the water vapor generated by the HL; s_{pen} is the operating state of the HL; m_{pen} is the spray volume of HL per unit time; α is the influence coefficient of the difference in water vapor pressure in the room on the rate of water evaporation; $T_{\text{in}}(t)$ is the indoor temperature at time t; $e'(T_{\text{in}}(t))$ is the saturation water vapor pressure at T_{in}; $e(T_{\text{in}}(t))$ is the actual water vapor pressure; $H_{\text{in}}(t)$ is the humidity in the greenhouse; $H_{\text{soil}}(t)$ is the water vapor evaporated from the soil surface; and $H_{\text{air}}(t)$ is the water vapor lost by ventilation.

$H_{\text{in}}(t)$ can be expressed as:

$$H_{\text{in}}(t)=h_{\text{avg}}\frac{\text{d}x_{\text{in}}(t)}{\text{d}t} \tag{4}$$

$$\begin{aligned}x_{\text{in}}(t)=x'_{\text{in}}(T_{\text{in}}(t))h_{\text{in}}(t)=\frac{M}{AT_{\text{in}}(t)}e'(T_{\text{in}}(t))h_{\text{in}}(t)=\\ \frac{M}{AT_{\text{in}}(t)}h_{\text{in}}(t)e_0\exp\left[\frac{17.27T_{\text{in}}(t)}{237.3+T_{\text{in}}(t)}\right]\end{aligned} \tag{5}$$

where h_{avg} is the average height of the greenhouse; $h_{in}(t)$ is the relative humidity of the greenhouse; $x_{in}(t)$ is the indoor water vapor density; $x'_{in}(T_{in}(t))$ is the saturated water vapor density when the greenhouse temperature is T_{in}; M is the molar mass of water, A is the ideal gas constant; and e_0 is the saturated water vapor pressure when the indoor temperature is 0 °C.

$H_{soil}(t)$ can be expressed as:

$$H_{soil}(t)=S_{soil}\beta\frac{1.86\left|T_{soil}(t)-T_{in}(t)\right|}{v_h\gamma}[e'(T_{in}(t))-e(T_{in}(t))] \tag{6}$$

where S_{soil} is the greenhouse soil area; β is the relative ground moisture; $T_{soil}(t)$ is the soil surface temperature; v_h is the latent heat of evaporation; and γ is the energy factor for water evaporation.

$H_{air}(t)$ primarily includes two components, natural ventilation H_n and fan ventilation H_f [31], and can be expressed as:

$$\begin{aligned}H_{air}(t)&=H_n(t)+H_f(t)=\\&G_n(t)(x_{in}(t)-x_{out}(t))+G_f(t)(x_{in}(t)-x_{out}(t))\end{aligned} \tag{7}$$

$$G_n(t)=S_{win}C_o\left[gh_{win}\frac{T_{in}(t)-T_{out}(t)}{2T_{out}(t)}+C_nW_{out}^2(t)\right]\sin\frac{\omega}{2} \tag{8}$$

where $G_n(t)$ is the natural ventilation rate of the greenhouse; $G_f(t)$ is the fan ventilation rate; $x_{out}(t)$ is the outdoor water vapor density; S_{win} is the greenhouse window area; ω is the greenhouse window opening angle; g is the acceleration due to gravity; h_{win} is the vertical height of the skylight; C_o is the flow coefficient; C_n is the integrated wind pressure coefficient; and $W_{out}(t)$ is the outdoor wind speed.

In summary, the model of HLs such as sprayers can be expressed as:

$$P_{pen}(t)=s_{pen}(t)P_{pen}=\frac{H_{in}(t)-H_{soil}(t)-H_{air}(t)}{m_{pen}\alpha[e'(T_{in}(t))-e(T_{in}(t))]}P_{pen} \tag{9}$$

$$s_{pen}(t)=\begin{cases}0, & x_{in}(t)\geqslant x_{in,max}\\1, & x_{in}(t)\leqslant x_{in,min}\\s_{pen}(t-\varepsilon), & \text{others}\end{cases} \tag{10}$$

where $P_{pen}(t)$ is the actual power of the HL; P_{pen} is the rated power of the HL; $s_{pen}(t)$ is the operating state of TL; whereas $s_{pen}(t)$ is 1 and 0 imply that the TL is online and offline, respectively; and ε is the sampling interval.

3) Temperature-controlled Load Model

Greenhouse temperature is primarily influenced by solar radiation, heat exchange with external ventilation, and heating equipment. According to the energy balance, the TL model can be established as follows:

$$V_{gh}\rho C_{air}\frac{dT_{in}(t)}{dt}=Q_{rad}(t)+Q_{air}(t)+Q_{heat}(t) \tag{11}$$

$$Q_{rad}(t)=S_mI_{out}(t)\tau_r \tag{12}$$

$$Q_{air}(t)=\rho_oC_{air}(T_{in}(t)-T_{out}(t))(G_n(t)+G_f(t)) \tag{13}$$

$$Q_{heat}(t)=\eta_{heat}P_{heat}s_{heat}(t) \tag{14}$$

where V_{gh} is the greenhouse volume; ρ is the density of greenhouse air; $Q_{rad}(t)$ is the heat from solar radiation; $Q_{air}(t)$ is the heat from ventilation exchange; $Q_{heat}(t)$ is the heat from TL; S_m is the greenhouse cover area; τ_r is the total material light transmission; ρ_o is the density of outdoor air; C_{air} is the specific heat capacity of air; P_{heat} is the rated power of TL; η_{heat} is the energy efficiency ratio; and $s_{heat}(t)$ is the operating state of the TL, whereas $s_{heat}(t)$ is 1 and 0 imply that the TL is in and out of operation, respectively.

From the growth characteristics of different crops, TL can realize indoor temperature control by relative state start/stop as follows:

$$s_{heat}(t)=\begin{cases}0, & T_{in}(t)\geqslant T_{in,max}\\1, & T_{in}(t)\leqslant T_{in,min}\\s_{heat}(t-\varepsilon), & \text{others}\end{cases} \tag{15}$$

$$P_{heat}(t)=P_{heat}s_{heat}(t) \tag{16}$$

For other flexible loads such as plasma nitrogen fixation, and with nutrient sterilizer, the load power is the rated power. Hence, they are not modeled separately.

III. Parameter Identification Based on RLS

The majority of the parameters in the aforementioned load models can be obtained by sensors and regional meteorological data. However, the direct determination of some building thermodynamic and crop state parameters in the HL and TL models is difficult. Therefore, this section proposes a parameter identification method for HLs and TLs based on RLS.

A. Parameter Identification Models

1) Parameter Identification of HL

Humidity variation can be obtained by integrating (9) from t_p to t_q and separating the constant parameters from the time-varying parameters, as:

$$\begin{aligned}m_{pen}\alpha\int_{t_p}^{t_q}N_{pen}(t)[e'(T_{in})-e(T_{in})]dt&=h_{avg}[x_{in}(t_q)-x_{in}(t_p)]-\\1.86S_{soil}\beta\int_{t_p}^{t_q}&\frac{\left|T_{soil}-T_{in}\right|}{v_h(T_{in})\gamma}[e'(T_{in})-e(T_{in})]dt-\\\int_{t_p}^{t_q}&(G_n+G_f)[x_{in}(t)-x_{out}(t)]dt\end{aligned} \tag{17}$$

where N_{pen} is the number of HLs.

Assuming the sampling interval of each data to be ε, the parameter identification expression of HLs can be obtained by discretizing (17) as:

$$K_1X_1(t) = Y_{\text{H}} - K_2X_2 - K_3X_3 - K_4X_4 - K_5X_5 \quad (18)$$

where the parameters and variables to be solved are as (19) and (20), respectively:

$$\begin{cases} K_1 = m_{\text{pen}}\alpha \\ K_2 = \dfrac{1.86S_{\text{soil}}\beta e_0}{\gamma} \\ K_3 = S_{\text{win}}C_o g h_{\text{win}} \sin\dfrac{\omega}{2} \\ K_4 = S_{\text{win}}C_{\text{o}}C_{\text{n}} \sin\dfrac{\omega}{2} \\ K_5 = C_{\text{n}}P_{\text{f}} \end{cases} \quad (19)$$

$$\begin{cases} Y_{\text{H}} = h_{\text{avg}}[x_{\text{in}}(t_q) - x_{\text{in}}(t_p)] \\ X_1 = \varepsilon\sum_{t=t_p}^{t_{q-1}} N_{\text{pen}}(t)[1-h_{\text{in}}(t)]\exp\left(\dfrac{17.27T_{\text{in}}}{237.3+T_{\text{in}}}\right) \\ X_2 = \varepsilon\sum_{t=t_p}^{t_{q-1}} \dfrac{\left|T_{\text{soil}} - T_{\text{in}}\right|[1-h_{\text{in}}(t)]}{v_{\text{h}}(T_{\text{in}})}\exp\left(\dfrac{17.27T_{\text{in}}}{237.3+T_{\text{in}}}\right) \\ X_3 = \varepsilon\sum_{t=t_p}^{t_{q-1}} \dfrac{T_{\text{in}} - T_{\text{out}}}{2T_{\text{out}}}[x_{\text{in}}(t) - x_{\text{out}}(t)] \\ X_4 = \varepsilon\sum_{t=t_p}^{t_{q-1}} W_{\text{out}}^2(t)[x_{\text{in}}(t) - x_{\text{out}}(t)] \\ X_5 = \varepsilon\sum_{t=t_p}^{t_{q-1}} s_{\text{f}}(t)W_{\text{f}}(t)[x_{\text{in}}(t) - x_{\text{out}}(t)] \end{cases} \quad (20)$$

where s_{f} is the operating status of the fan; W_{f} is the wind speed of the fan; the values of x_{in}, h_{in}, x_{out}, T_{in}, T_{out}, T_{soil}, and W_{out} can be obtained from sensors and basic meteorological data, whereas the values of N_{pen} and s_{f} can be obtained from the equipment operational data. Therefore, K1–K4 are the parameters to be identified.

2) Parameter Identification of TL

The temperature change equilibrium can be expressed by integrating Eqs. (11)–(15) from t_p to t_q as:

$$\begin{aligned} &V_{\text{gh}}\rho C_{\text{air}}[T_{\text{in}}(t_q) - T_{\text{in}}(t_p)] = S_{\text{m}}\tau_r\int_{t_p}^{t_q} I_{\text{out}}(t)\text{d}t + \\ &\rho_{\text{o}}C_{\text{air}}\int_{t_p}^{t_q}[T_{\text{in}}(t) - T_{\text{out}}(t)][G_{\text{n}}(t) + G_{\text{f}}(t)]\text{d}t + \\ &\eta_{\text{heat}}P_{\text{heat}}\int_{t_p}^{t_q} s_{\text{heat}}(t)\text{d}t \end{aligned} \quad (21)$$

Assuming the sampling interval of each data to be ε, the parameter identification expression of TLs can be obtained by discretizing (21) as follows:

$$Y_{\text{T}} = M_1Z_1 + M_2Z_2 + M_3Z_3 + M_4Z_4 + M_5Z_5 \quad (22)$$

where the parameters to be determined are shown in (23) and the variables are presented by (24):

$$\begin{cases} M_1 = \dfrac{S_{\text{m}}\tau_r}{V_{\text{gh}}\rho C_{\text{air}}} \\ M_2 = \dfrac{S_{\text{win}}C_{\text{o}}gh\sin\dfrac{\omega}{2}}{V_{\text{gh}}} \\ M_3 = \dfrac{S_{\text{win}}C_{\text{o}}C_{\text{n}}\sin\dfrac{\omega}{2}}{V_{\text{gh}}} \\ M_4 = \dfrac{P_{\text{f}}}{V_{\text{gh}}} \\ M_5 = \dfrac{1}{\rho C_{\text{air}}V_{\text{gh}}} \end{cases} \quad (23)$$

$$\begin{cases} Y_{\text{T}} = [T_{\text{in}}(t_q) - T_{\text{in}}(t_p)] \\ Z_1 = \varepsilon\sum_{t=t_p}^{t_{q-1}} I_{\text{out}}(t) \\ Z_2 = \varepsilon\sum_{t=t_p}^{t_{q-1}} \dfrac{[T_{\text{in}}(t) - T_{\text{out}}(t)]^2}{2T_{\text{out}}} \\ Z_3 = \varepsilon\sum_{t=t_p}^{t_{q-1}} W_{\text{out}}^2(t)[x_{\text{in}}(t) - x_{\text{out}}(t)] \\ Z_4 = \varepsilon\sum_{t=t_p}^{t_{q-1}} s_{\text{f}}(t)W_{\text{f}}(t)[x_{\text{in}}(t) - x_{\text{out}}(t)] \\ Z_5 = \varepsilon\sum_{t=t_p}^{t_{q-1}} \eta_{\text{heat}}P_{\text{heat}}s_{\text{heat}}(t) \end{cases} \quad (24)$$

where the values of I_{out}, x_{in}, h_{in}, x_{out}, T_{in}, T_{out}, T_{soil}, and W_{out} can be obtained from sensors and basic meteorological data, whereas the values of s_{heat} and s_{f} can be obtained from equipment operational data. Therefore, M1–M5 are the parameters to be identified.

B. Recursive Least Squares

The least squares (LS) method is commonly used for parameter identification [32]. However, as the dimensionality of the identified parameters increases, LS suffers from data saturation. Therefore, in this paper, a forgetting factor λ is introduced in the recursive formula to effectively deal with this problem. For $\boldsymbol{P}(k) = (\boldsymbol{\varphi}^{\text{T}}(k)\boldsymbol{\varphi}(k))^{-1}$, the corresponding recursive formula is expressed as:

$$\begin{cases} \boldsymbol{\theta}(k) = \boldsymbol{\theta}(k-1) + \boldsymbol{K}(k)\left[\boldsymbol{y}(k) - \boldsymbol{\varphi}^{\text{T}}(k-1)\boldsymbol{\theta}(k-1)\right] \\ \boldsymbol{K}(k) = \dfrac{\boldsymbol{P}(k-1)\boldsymbol{\varphi}(k-1)}{\lambda + \boldsymbol{\varphi}^{\text{T}}(k-1)\boldsymbol{P}(k-1)\boldsymbol{\varphi}(k-1)} \\ \boldsymbol{P}(k) = \dfrac{1}{\lambda}\left[I - \boldsymbol{K}(k)\boldsymbol{\varphi}^{\text{T}}(k-1)\right]\boldsymbol{P}(k-1) \end{cases} \quad (25)$$

where $\boldsymbol{\theta}(k)$ is the new parameter identification vector; $\boldsymbol{\theta}(k-1)$ is the previous recursive parameter identification vector; $\boldsymbol{K}(k)$ is the gain vector; $\boldsymbol{y}(k)$ is the output vector; $\boldsymbol{\varphi}(k)$ is the input vector; $\boldsymbol{P}(k)$ is the intermediate vector of correction; and λ is the forgetting factor with values most commonly between 0.9 and 1.0.

Applying RLS to model the parameter identification of the HL and TL, the corresponding linear equations are:

For HL:

$$\boldsymbol{\theta}_{\text{pen}}(k)=[\boldsymbol{K}_1(k)\quad \boldsymbol{K}_2(k)\quad \boldsymbol{K}_3(k)\quad \boldsymbol{K}_4(k)\quad 1]^{\text{T}} \tag{26}$$

$$\boldsymbol{\varphi}_{\text{pen}}(k)=[X_1(k)\quad X_2(k)\quad X_3(k)\quad X_4(k)\quad X_5(k)]^{\text{T}} \tag{27}$$

$$\boldsymbol{y}_{\text{pen}}(k)=Y_{\text{H}}(k)=\boldsymbol{\varphi}_{\text{pen}}^{\text{T}}(k)\boldsymbol{\theta}_{\text{pen}}(k) \tag{28}$$

For TL:

$$\boldsymbol{\theta}_{\text{heat}}(k)=[M_1(k)\ M_2(k)\ M_3(k)\ M_4(k)\ M_5(k)]^{\text{T}} \tag{29}$$

$$\boldsymbol{\varphi}_{\text{heat}}(k)=[Z_1(k)\ Z_2(k)\ Z_3(k)\ Z_4(k)\ Z_5(k)]^{\text{T}} \tag{30}$$

$$y_{\text{heat}}(k)=Y_{\text{T}}(k)=\boldsymbol{\varphi}_{\text{heat}}^{\text{T}}(k)\boldsymbol{\theta}_{\text{heat}}(k) \tag{31}$$

IV. Optimal Aggregation Model for GHLs

The load characteristics of GHLs vary significantly based on the different types of greenhouse crops. Performing a single aggregation for all GHLs at longer time scales increases algorithm complexity and solution time, resulting in the park's inability to provide continuous and reliable responses. Therefore, this paper proposes a calculation method for the regulation potential of GHLs and establishes the optimization aggregation model considering the day-ahead optimization aggregation of GHLs as an example.

A. Assessment of Load Regulation Potential

1) Regulation Potential Model of LL

Whether the LL has regulation potential at a certain moment can be determined by the daily light integral (DLI) as follows:

$$DLI(t)=\left[\sum_{t=1}^{T}\frac{P_{\text{light}}(t)s_{\text{light}}(t)\eta_{\text{light}}}{S_{\text{gh}}\phi_0 C_1 C_2}+\sum_{t=1}^{T}\lambda I_{\text{out}}(t)\right]\times\frac{3600}{10^6} \tag{32}$$

$$C_{\text{light,re}}^{n}(t)=\begin{cases}P_{\text{light}} & DLI(t)\geqslant DLI_{\min}\\ 0 & DLI(t)<DLI_{\min}\end{cases} \tag{33}$$

where s_{light} is the operating state of the LL; $DLI_{\min}$ is the DLI boundary threshold and $C_{\text{light,re}}^{i}$ is the regulation capacity of the nth LL.

Accordingly, the maximum regulation capacity of the LL in the agricultural park is:

$$C_{\text{light,re}}(t)=\sum_{n=1}^{N_{\text{light}}}C_{\text{light,re}}^{n} \tag{34}$$

where N_{light} is the number of LLs.

2) Regulation Potential Model of HL

An HL can achieve rapid load reduction by appropriately varying the humidity setting value without affecting the crop-growing conditions [33]. Indoor and outdoor temperatures, outdoor water vapor density, soil temperature, and outdoor wind speed are assumed to be constant during the regulation time period. Based on (17)–(20), the switching time of the HL from xin1 to xin2 can be calculated using (35) and (36).

$$\tau_{\text{pen,on}}(x_{\text{in1}},x_{\text{in2}})=\frac{1}{h_{\text{avg}}(K_3\frac{T_{\text{in}}-T_{\text{out}}}{2T_{\text{out}}}+K_4W_{\text{out}}^2+s_{\text{f}}W_{\text{f}})}\times \ln\left(\frac{[K_1+K_2\frac{|T_{\text{soil}}-T_{\text{in}}|}{v_{\text{h}}(T_{\text{in}})}][e'(T_{\text{in}})-e(T_{\text{in}})]+(K_3\frac{T_{\text{in}}-T_{\text{out}}}{2T_{\text{out}}}+K_4W_{\text{out}}^2+s_{\text{f}}W_{\text{f}})(x_{\text{in2}}-x_{\text{out}})}{[K_1+K_2\frac{|T_{\text{soil}}-T_{\text{in}}|}{v_{\text{h}}(T_{\text{in}})}][e'(T_{\text{in}})-e(T_{\text{in}})]+(K_3\frac{T_{\text{in}}-T_{\text{out}}}{2T_{\text{out}}}+K_4W_{\text{out}}^2+s_{\text{f}}W_{\text{f}})(x_{\text{in1}}-x_{\text{out}})}\right) \tag{35}$$

$$\tau_{\text{pen,off}}(x_{\text{in1}},x_{\text{in2}})=\frac{1}{h_{\text{avg}}(K_3\frac{T_{\text{in}}-T_{\text{out}}}{2T_{\text{out}}}+K_4W_{\text{out}}^2+s_{\text{f}}W_{\text{f}})}\times \ln\left(\frac{K_2\frac{|T_{\text{soil}}-T_{\text{in}}|[e'(T_{\text{in}})-e(T_{\text{in}})]}{v_{\text{h}}(T_{\text{in}})}+(K_3\frac{T_{\text{in}}-T_{\text{out}}}{2T_{\text{out}}}+K_4W_{\text{out}}^2+s_{\text{f}}W_{\text{f}})(x_{\text{in2}}-x_{\text{out}})}{K_2\frac{|T_{\text{soil}}-T_{\text{in}}|[e'(T_{\text{in}})-e(T_{\text{in}})]}{v_{\text{h}}(T_{\text{in}})}+(K_3\frac{T_{\text{in}}-T_{\text{out}}}{2T_{\text{out}}}+K_4W_{\text{out}}^2+s_{\text{f}}W_{\text{f}})(x_{\text{in1}}-x_{\text{out}})}\right) \tag{36}$$

where $\tau_{\text{pen,on}}$ and $\tau_{\text{pen,off}}$ are the operating and closing times of the HL, respectively. Based on the humidity setting range $[x_{\min},x_{\max}]$, the maximum continuous operating time $\tau_{\text{pen,on}}(x_{\min},x_{\max})$, and the maximum continuous closing time $\tau_{\text{pen,off}}(x_{\min},x_{\max})$, the control cycle $\tau_{\text{pen,c}}$ is:

$$\tau_{\text{pen,c}}=\tau_{\text{pen,on}}+\tau_{\text{pen,off}} \tag{37}$$

The maximum regulation capacity of HLs can thus be calculated as:

$$C_{\text{pen,re}}(t)=\frac{\tau_{\text{pen,off}}}{\tau_{\text{pen,c}}}\times N_{\text{pen}}P_{\text{pen}} \tag{38}$$

3) Regulation Potential Model of TL

Similar to HL, a TL can also achieve rapid load reduction by appropriately varying the temperature setting value [34]. The outdoor temperature, outdoor radiation flux, indoor and outdoor water vapor densities, and

outdoor wind speed are assumed to be constant during temperature regulation. Based on (21)–(24), the switching time of TL from T_1 to T_2 can be calculated using (39) and (40).

$$\tau_{\text{heat,on}}(T_1,T_2)=\frac{1}{\sqrt{2T_{\text{out}}M_2}}\times\text{In}\left(\frac{M_1I_{\text{out}}+M_2\dfrac{(T_2-T_{\text{out}})^2}{T_{\text{out}}}+(M_3W_{\text{out}}^2+M_4s_{\text{f}}W_{\text{f}})(x_{\text{in}}-x_{\text{out}})+M_5}{M_1I_{\text{out}}+M_2\dfrac{(T_1-T_{\text{out}})^2}{T_{\text{out}}}+(M_3W_{\text{out}}^2+M_4s_{\text{f}}W_{\text{f}})(x_{\text{in}}-x_{\text{out}})+M_5}\right) \tag{39}$$

$$\tau_{\text{heat,off}}(T_1,T_2)=\frac{1}{\sqrt{2T_{\text{out}}M_2}}\times\text{In}\left(\frac{M_1I_{\text{out}}+M_2\dfrac{(T_2-T_{\text{out}})^2}{T_{\text{out}}}+(M_3W_{\text{out}}^2+M_4s_{\text{f}}W_{\text{f}})(x_{\text{in}}-x_{\text{out}})}{M_1I_{\text{out}}+M_2\dfrac{(T_1-T_{\text{out}})^2}{T_{\text{out}}}+(M_3W_{\text{out}}^2+M_4s_{\text{f}}W_{\text{f}})(x_{\text{in}}-x_{\text{out}})}\right) \tag{40}$$

where $\tau_{\text{heat,on}}$ and $\tau_{\text{heat,off}}$ are the operating and closing times of the TL, respectively. Based on the temperature setting range $[T_{\min},T_{\max}]$, the maximum continuous operating time $\tau_{\text{heat,on}}(T_{\min},T_{\max})$, and the maximum continuous closing time $\tau_{\text{heat,off}}(T_{\min},T_{\max})$, the control cycle $\tau_{\text{heat,c}}$ is:

$$\tau_{\text{heat,c}}=\tau_{\text{heat,on}}+\tau_{\text{heat,off}} \tag{41}$$

The maximum regulation capacity of the TLs can thus be calculated as:

$$C_{\text{heat,re}}(t)=\frac{\tau_{\text{heat,off}}}{\tau_{\text{heat,c}}}N_{\text{heat}}P_{\text{heat}} \tag{42}$$

where N_{heat} is the number of TLs.

4) Response Potential Model of Other Loads

Agricultural greenhouses contain not only LLs, HLs, and TLs but also many other flexible loads, such as submersible pumps, plasma nitrogen fixation, water and fertilizer integration, and nutrient sterilizers 0. These loads have fast response time and simple control when regulated. According to the load characteristics, their regulation capacity can be assessed as:

$$C_{\text{FLu,re}}(t)=\sum_{n=1}^{N_{\text{FLi}}}s_{\text{FLu},n}(t)P_{\text{FLu},n} \tag{43}$$

where $C_{\text{FLu,re}}(t)$ is the regulation capacity of the flexible load I; N_{FLi} is the number of flexible loads; $s_{\text{FLu},n}(t)$ is the operating state of the nth load in the flexible load; and $P_{\text{FLu},n}$ is the rated power of the flexible load.

B. Optimal Aggregation Model for GHLs

Using the minimum total daily regulation cost as the objective function, flexible loads with lower regulation costs are prioritized for aggregation by setting the weighting factor as follows:

$$\begin{aligned}&\min F_{\text{DR}}=\min\sum_k\sum_i\sum_t\omega_kF_{i,\text{DR}}C_{i,\text{re}}(t)\lambda_{i,k},\\&C_{i,\text{re}}\in[C_{\text{light,re}},C_{\text{pen,re}},C_{\text{heat,re}},C_{\text{FLu,re}}]\end{aligned} \tag{44}$$

where $F_{i,\text{DR}}$ is the unit regulation cost of load I; $C_{i,\text{re}}$ is the maximum regulation capacity of load I; $\lambda_{i,k}$ is the affiliation status of load i with aggregator k; and ω_k is the weighting factor of aggregator k.

C. Constraints

1) Load Aggregate Frequency Constraint

Each load can only be allocated to one aggregator, i.e.:

$$\sum_k\lambda_{i,k}\leqslant 1 \tag{45}$$

2) Load Coupling Constraint

In the case where loads, such as a submersible pump (load p) and a translational sprinkler (load q), have a coupling relationship, where the translational sprinkler cannot operate without water supply from the submersible pump, it is essential to assign both of them to the same aggregator during aggregation, as:

$$\lambda_{p,k}-\lambda_{q,k}=0,\quad p,q\in\phi_{\text{couple}} \tag{46}$$

where $\lambda_{p,k}$ and $\lambda_{q,k}$ is the affiliation status of load p and q with aggregator k; and ϕ_{couple} is the set of loads with a coupling relationship.

3) Regulation Capacity Constraint

To fully explore the regulation capacity of aggregators, the regulation capacity of each aggregator should be larger than the minimum aggregation capacity $C_{\text{min,re}}$, i.e.:

$$\sum_i\sum_t C_{i,\text{re}}(t)\lambda_{i,k}\geqslant C_{\text{min,re}} \tag{47}$$

4) Greenhouse Environmental Constraints

The temperature, humidity, and light of each greenhouse must meet the requirements for crop growth, i.e.:

$$T_{\min}\leqslant T_{\text{in}}(t)\leqslant T_{\max} \tag{48}$$

$$x_{\min}\leqslant x_{\text{in}}(t)\leqslant x_{\max} \tag{49}$$

$$DLI_{\min}\leqslant DLI(t)\leqslant DLI_{\max} \tag{50}$$

V. Results and Discussion

We consider a modern agricultural park in December as an example of load aggregation. The regulation potential is analyzed between 8:00 to 22:00. The topology of the agricultural park, as shown in Fig. 1, primarily comprises ten greenhouses and an information control

center. The park is connected to the distribution network externally, and internal GHLs can be controlled by the information control center.

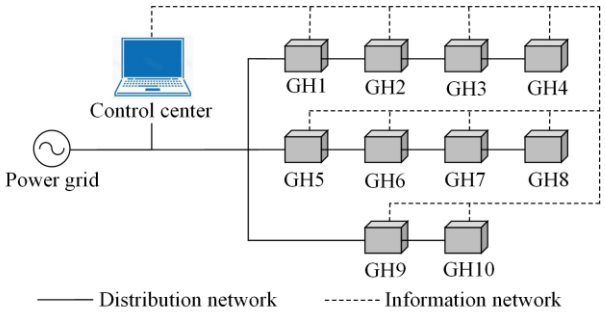

Fig. 1. Topological structure of a modern agricultural park.

For analysis and calculation, all the greenhouses are assumed to have the same volume, crop growing area, etc. The relevant parameters are listed in Table II.

TABLE II
GREENHOUSE-RELATED PARAMETERS

Parameter	Value
S_{gh}	50000 m^2
h_{avg}	6 m
γ	66 Pa/K

The types of flexible loads contained within the agricultural park with their corresponding numbers are listed in Table III. In each greenhouse, the load characteristics vary slightly because of different crop types, and the flexible load configurations for each greenhouse are shown in Fig. 2.

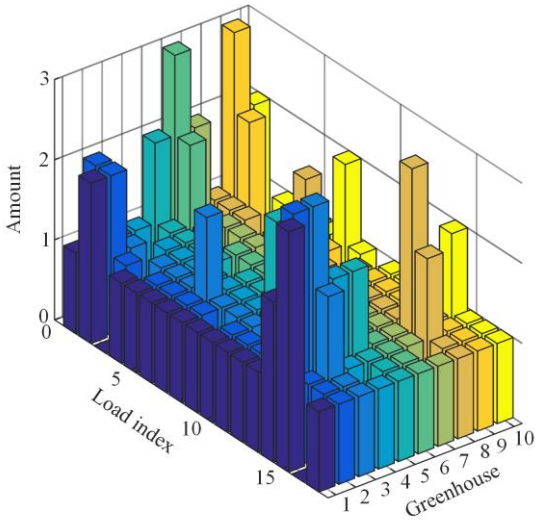

Fig. 2. Load configurations for different greenhouses.

TABLE III
TYPES AND REGULATION PARAMETERS OF GHLS IN THE PARK

No.	Load type	Maximum response duration (min)	Minimum recovery time (min)	Response cost (¥/kWh)	Daily response capacity (kWh)
L1	LED lighting	60	15	0.25	308.7
L2	Microwave sulfur lamp	60	15	0.25	270
L3	Sound wave booster	60	15	0.25	227.5
L4	Negative air pressure machine	30	15	0.3	312.5
L5	Circulating ventilator	30	15	0.3	350.4
L6	Fans coil	20	10	0.3	320
L7	Electric shock insecticidal lamp	30	15	0.25	111.6
L8	Plasma nitrogen fixation	45	20	0.35	234.4
L9	Space electric field	30	15	0.35	350
L10	Water & Fertilizer integration	30	15	0.3	151.5
L11	Organic fertilizer dispenser	45	20	0.3	247.5
L12	Nutrient sterilizer	30	15	0.3	250
L13	Submersible pump	30	15	0.25	312.36
L14	Panning water sprinkler	12	9	0.25	191.23
L15	Carbon crystal electric heating panel	11	8	0.3	475.46
L16	Far infrared heating	11	8	0.35	314.59
L17	Cleaning equipment	30	15	0.35	320

A. Model Parameter Identification

Owing to the different characteristics of the greenhouses, the temperature and humidity ranges vary considerably, as presented in Table IV.

Historical data of the control cycles and power curves of the HL and TL in each greenhouse are shown in Fig. 3.

According to the aforementioned HL and TL models, to identify building thermodynamic and crop state parameters that cannot be obtained conveniently, the environmental data and operational state collected within 24 hours are used as input. Subsequently, after an identification period of 1 h, the model parameters of the HL and TL can be identified according to (17)–(24). Considering GH1 as an example, the parameter identification results of the HL and TL from 08:00 to 22:00 are presented respectively in Tables AI and AII in the Appendix A.

TABLE IV
ENVIRONMENTAL SETTING RANGES OF GREENHOUSES

Greenhouse	T_{min} (℃)	T_{max} (℃)	x_{min} (%)	x_{max} (%)
GH1	23	26	66	69
GH2	15	18	81	84
GH3	23	26	85	87
GH4	8	11	62	65
GH5	15	18	71	74
GH6	13	16	56	59
GH7	15	18	51	54
GH8	20	23	81	84
GH9	17	20	54	57
GH10	10	13	61	64

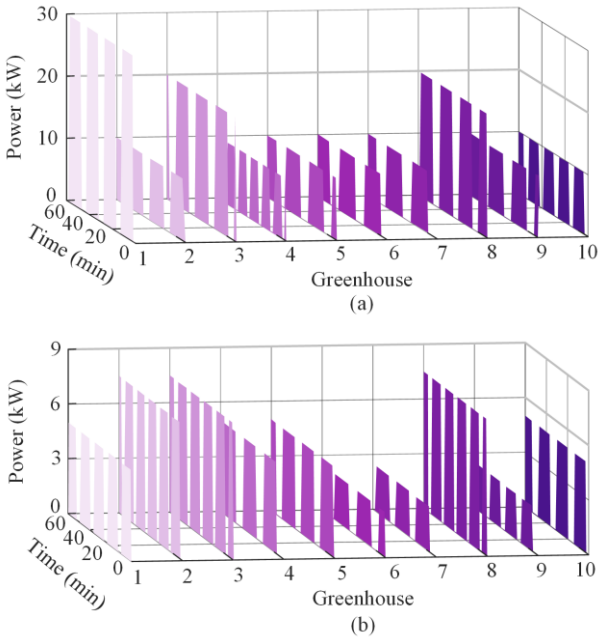

Fig. 3. Control cycles and power curves of the HL and TL. (a) Power of HL. (b) Power of TL.

B. Regulation Capability Analysis

HL and TL can achieve rapid load reduction/increase by adjusting the humidity level without affecting the growing conditions of the crop.

From the results of parameter identification, considering 19:00 as an example, upon combining (35), (36) and (37), (38), T_{max} and x_{max} can be adjusted both upward and downward by 1 °C and 2 °C each. In addition, the power curves of the TLs and HLs can be calculated, as shown in Figs. 4 and 5, respectively.

As observed from Figs. 4 and 5, the load power of the TL and HL can be effectively reduced/increased by adjusting the setting values of T_{max}/x_{max} downward/upward. When T_{max} is adjusted downward by 1 °C, upward by 1 °C, downward by 2 °C, and upward by 2 °C, the average power consumed is 78 kW, 87.5 kW, 74 kW, and 93.67 kW, respectively.When x_{max} is adjusted downward by 1%, upward by 1%, downward by 2%, and upward by 2%, the average power consumed is 29.96 kW, 31.71 kW, 28.5 kW, and 32.33 kW, respectively.

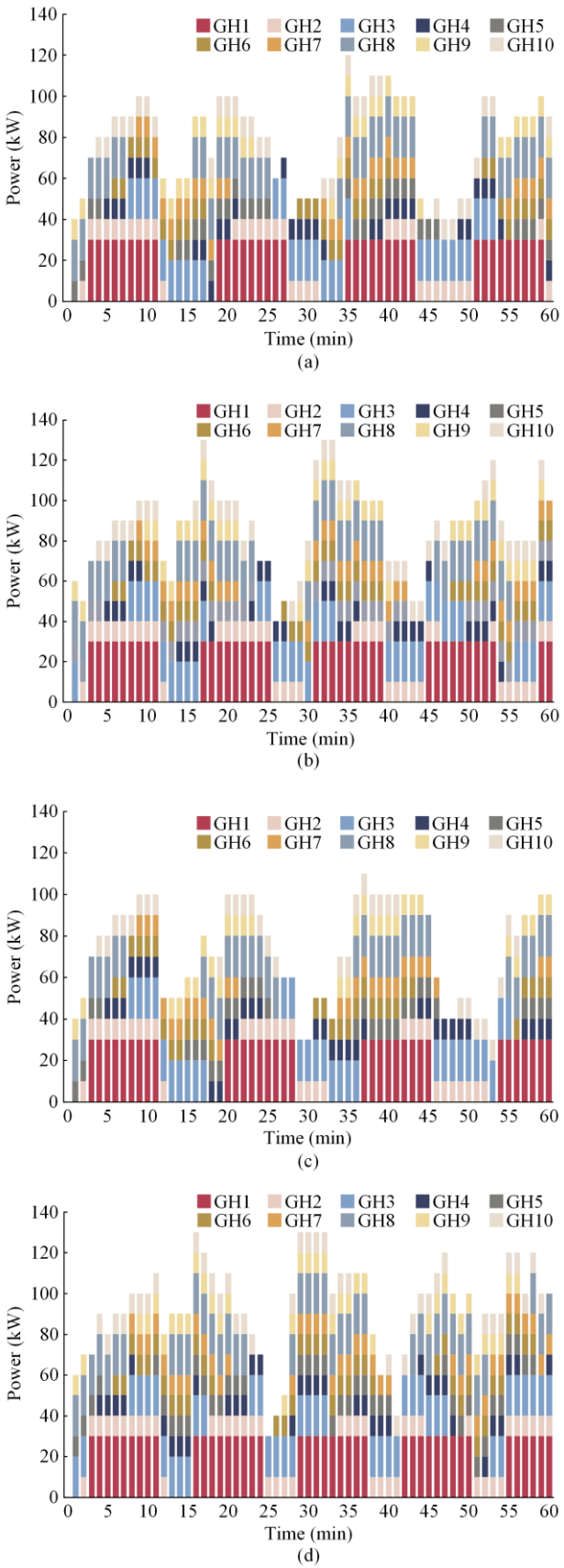

Fig. 4. Load demand of TL for different controlling parameters. (a) Downward by 1 ℃. (b) Upward by 1 ℃. (c) Downward by 2 ℃. (d) Upward by 2 ℃.

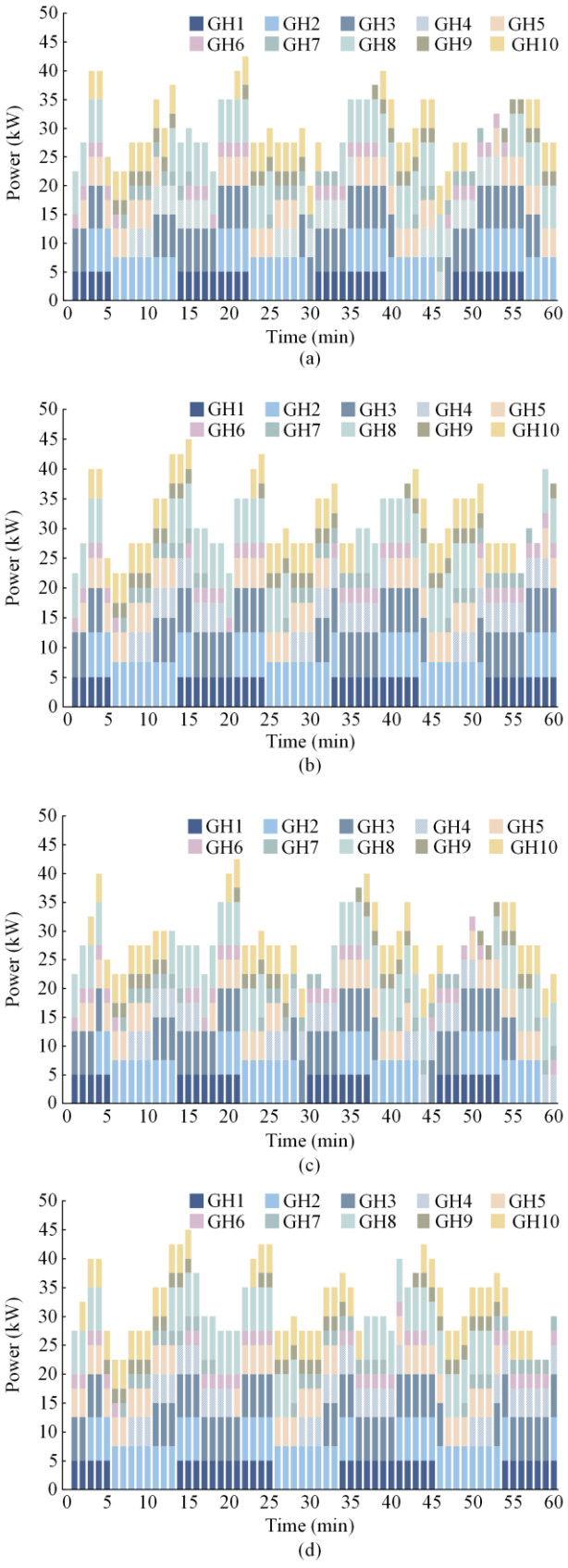

Fig. 5. Load demand of HL for different controlling parameters. (a) Downward by 1℃. (b) Upward by 1 ℃. Downward by 2℃. (d) Upward by 2℃.

This demonstrates that during peak electricity consumption in winter, adjusting the setting value of the HL and TL results in a regulation potential of 5%–10%. However, because of the influence of external temperature, humidity, and other factors, the regulation potential of each HL and TL varies from time to time and must be updated dynamically and periodically based on real-time environmental parameters and load operational data.

Considering peak regulation as an example, the upper temperature/humidity setting of each greenhouse is adjusted downward by 1 ℃/1%. Further, each load is assumed to be continuously regulated under ideal conditions. Combining (32)–(43) and the data from the electricity consumption of the previous day, the maximum power cut curve of each load can be calculated separately, as shown in Fig. 6.

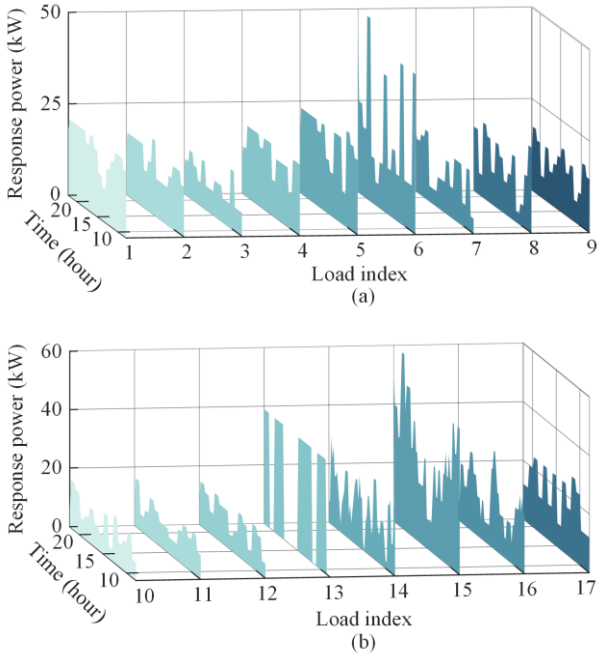

Fig. 6. Maximum cut power curve of each load. (a) for L1–L9. (b) for L10–L17.

Figure 6 illustrates that: 1) under ideal conditions, the carbon crystal electric heating panel has the largest regulation capacity. It has peaks in the morning and evening; 2) for the HL and TL, the power reductions are high with large fluctuations which enable rapid load reduction capability; and 3) for other flexible loads such as plasma nitrogen fixation equipment, water and fertilizer integration equipment, etc., the values of power reduction are lower but the fluctuations are milder than HL and TL, enabling them to achieve a continuous and reliable regulation response.

Based on the above calculation results, the daily reduction capacity of each load can be calculated, as shown in the last column of Table II.

C. Optimal Aggregation of GHLs

We set the number of aggregators to 3, and the weight factors are 0.4, 0.35, and 0.25. Then, the allocation of GHLs is obtained by analyzing the optimal aggregation model using CPLEX, as shown in Fig. 7.

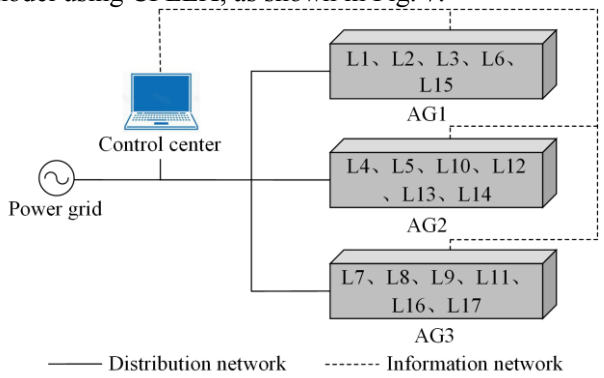

Fig. 7. Results of load aggregation.

From the results in Table IV, the daily regulation capacity and regulation cost of each aggregator can be calculated, as presented in Table V.

TABLE V
DAILY REGULATION CAPACITY AND COST OF AGGREGATORS

	AG1	AG2	AG3
Load index	L1、L2、L3、L6、L15	L4、L5、L10、L12、L13、L14	L7、L8、L9、L11、L16、L17
Regulation capacity (kWh)	1601.66	1567.99	1578.09
Regulation cost (¥)	440.188	445.2175	528.7965

The above optimization results show that some loads with higher regulation capacity and lower regulation costs (such as carbon crystal heating panels, negative air pressure machines, and LED lighting) are allocated to AG1 with priority during demand response. In contrast, loads with high regulation costs (such as plasma nitrogen fixation, space electric field, and far infrared heating,) are allocated to AG3 with a lower weighting factor.

The submersible pump and translational sprinkler with a coupling relationship are allocated simultaneously to AG2, to avoid the lack of water supply to the translational jets in the event that the submersible pumps stop operating, thereby complying with the load coupling constraint.

The instantaneous maximum power reduction curves of the aggregators are plotted in Fig. 8. As seen, the power reduction of AG1 fluctuates significantly, whereas the power reduction of AG3 fluctuates gently. This is because the power of the loads such as LED lightings and carbon crystal electric heating panels contained in AG1 is more affected by weather than the others. Between 11:00 and 15:00 the load power decreases as light and temperature rise, while at night, when light and temperature are both insufficient, the load power gradually increases, thereby increasing regulation potential.

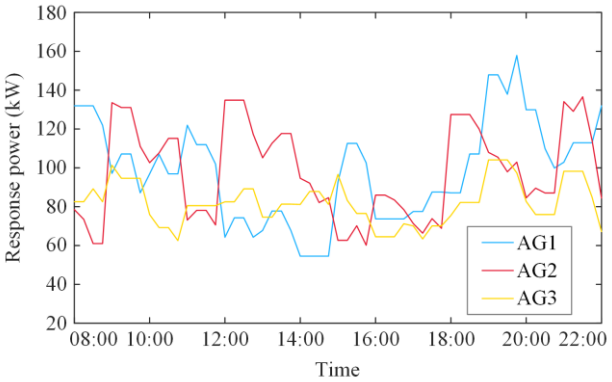

Fig. 8. Instantaneous maximum power reduction curves of aggregators.

Based on the above optimized aggregation results, the agricultural parks are regulated as an aggregator during intra-day dispatch. After receiving the regulation requirements from the grid, the control center sends control instructions to the configured AG1, AG2, and AG3 in order of priority. The ILs with regulation potential are taken out of operation, and the operational state of the HL and TL is controlled based on $\tau_{pen,c}$ and $\tau_{heat,c}$, thus meeting the grid dispatch capacity.

Taking peak regulation between 19:00 and 20:00 as an example, the load power curves after the participation of different aggregators in regulation are illustrated in Fig. 9.

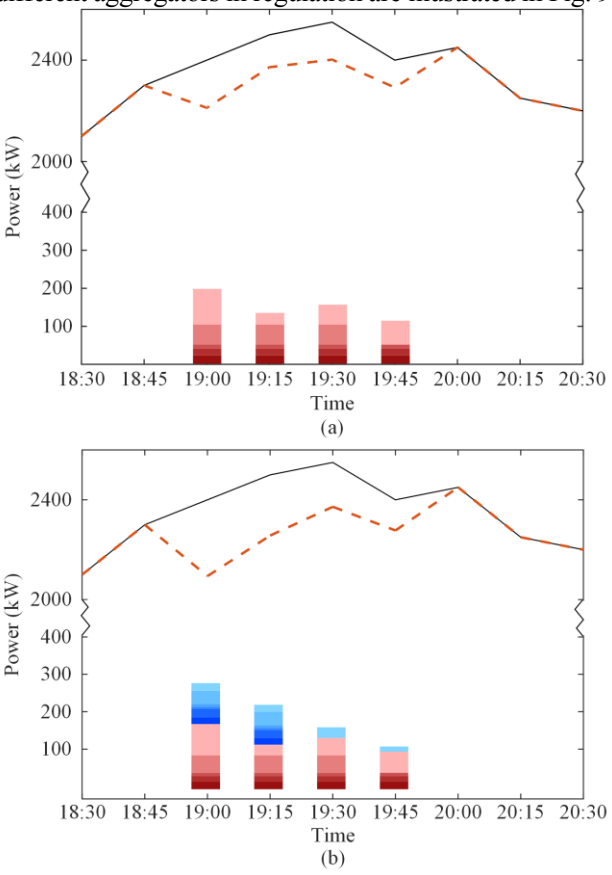

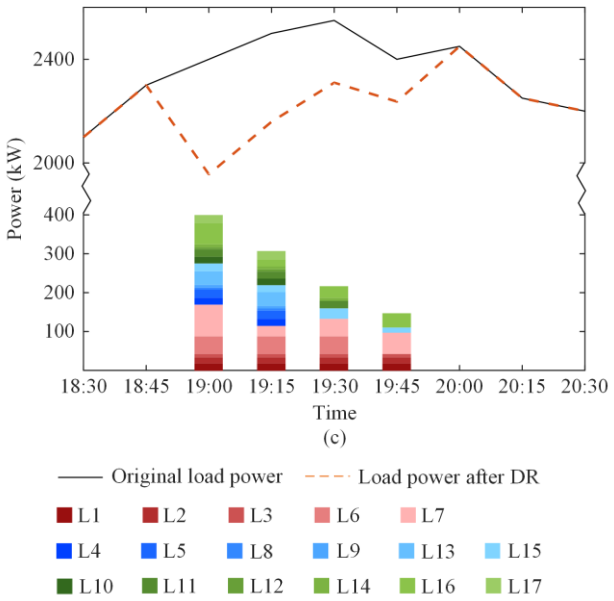

Fig. 9. Load power curves for different aggregators participating in energy regulation. (a) AG1 participates in DR. (b) AG1 and AG2 participate in DR. (c) AG1, AG2 and AG3 participate in DR.

As seen, the maximum power reductions in the three scenarios are 187.9 kW, 305.85 kW, and 443.47 kW, respectively. This, demonstrates the effective reduction of peak power consumption and relief of the pressure of peak load shifting. This proves the effectiveness of the regulation potential assessment model and optimal aggregation strategy of GHLs of an agricultural park.

VI. Conclusion

In this study, a detailed load demand model of GHLs is presented with the corresponding key parameters identified via RLS. Based on the quantitative evaluation of the regulation flexibility of GHLs, typical GHLs in the agricultural energy internet are optimally allocated to multiple flexible aggregators to explore their operational flexibility in supporting distribution grid power balance. The following conclusions can be drawn from the case study and discussion:

1) The detailed load demand models of GHLs can effectively support the regulation flexibility assessment of the GHLs participating in agricultural energy management.

2) The proposed RLS-based parameter identification method can effectively determine key parameters of GHL load models. Based on the parameter identification results, the load control cycles of the GHLs can be adjusted via parameter sensitivity analysis.

3) The proposed optimal aggregated aggregators can alleviate the peak load regulation pressure of power grids by flexibly shifting the load demands of the GHLs.

However, the assessment of the load reduction capacity of GHLs in this paper is based on the greenhouse environmental constraints. When GHLs participate in power regulation, their initial operating state changes, which in turn will affect the time-varying characteristics of the subsequent load reduction capacity. Therefore, further work will focus on performing the dynamic identification and correction of the load model parameters to update the reduction capacity of GHLs in real time. In addition, the established flexibility assessment model requires a large volume of load operation parameters and environmental data. However, obtaining these data may be expensive, laborious and difficult, and this may limit the generalization of the model. Therefore, how to realize a digitization twin for agricultural systems is a challenge that needs to be addressed.

Appendix A

TABLE AI
Parameter Identification Results of HL in GH1

Time	K1	K2	K3	K4	K5
08:00	1.763	0.385	0.001	0.695	4.246
09:00	1.652	0.362	0.004	0.587	4.586
10:00	2.095	0.014	0.385	1.028	4.804
11:00	1.476	0.655	0.275	0.409	4.013
12:00	1.613	0.521	0.140	0.546	4.141
13:00	1.998	0.135	0.246	0.930	4.532
14:00	1.611	0.521	0.140	0.544	4.147
15:00	1.812	0.320	0.061	0.745	4.349
16:00	1.693	0.439	0.058	0.626	4.229
17:00	1.750	0.382	0.001	0.683	4.286
18:00	1.807	0.325	0.056	0.740	4.343
19:00	1.746	0.386	0.005	0.679	4.283
20:00	1.777	0.354	0.026	0.710	4.314
21:00	1.735	0.397	0.016	0.668	4.271
22:00	1.763	0.369	0.012	0.696	4.299

TABLE AII
Parameter Identification Results of TL in GH1

Time	M1	M2	M3	M4	M5
08:00	0.207	0.152	0.156	0.259	0.072
09:00	0.048	0.102	0.098	0.004	0.325
10:00	0.062	0.008	0.012	0.114	0.216
11:00	0.053	0.107	0.103	0.001	0.330
12:00	0.037	0.017	0.013	0.089	0.240
13:00	0.055	0.001	0.005	0.107	0.222
14:00	0.001	0.055	0.051	0.051	0.278
15:00	0.074	0.020	0.024	0.126	0.204
16:00	0.087	0.033	0.037	0.139	0.191
17:00	0.058	0.004	0.008	0.110	0.220
18:00	0.136	0.082	0.086	0.188	0.142
19:00	0.100	0.045	0.049	0.152	0.178
20:00	0.146	0.200	0.196	0.094	0.424
21:00	0.046	0.008	0.004	0.098	0.232
22:00	0.119	0.065	0.069	0.171	0.158

Acknowledgment

Not applicable.

Authors' Contributions

Shiwei Xia and Ting Wu: conceived the idea and supervised the research. Liuyang Cai and Mingze Tong:

proposed the aggregation strategy and drafted the manuscript. Peng Li and Xiang Gao: helped to revise the manuscript. All authors read and approved the final manuscript.

FUNDING

This work is supported in part by the Science and Technology Project of State Grid Corporation of China (No. 1400-202224249A-1-1-ZN), the National Natural Science Foundation of China (No. 52077075 and No. 72271068), the Foundations of Shenzhen and Technology Committee (No. GJHZ20210705141811036 and No. GXWD20220811151845006), the Major Science and Technology Special Projects in Xinjiang Autonomous Region (No. 2022A01007), and the Fundamental Research Funds for the Central Universities (No. 2023JC001).

AVAILABILITY OF DATA AND MATERIALS

Not applicable.

DECLARATIONS

Competing interests: The authors declare that they have no known competing financial interests or personal relationships that could have appeared to influence the work reported in this article.

AUTHORS' INFORMATION

Shiwei Xia received the Ph.D. degree in power systems from The Hong Kong Polytechnic University, Hong Kong, in 2014. Subsequently, he worked as a post-doctoral fellow at the Hong Kong Polytechnic University in 2016. He was a visiting faculty member of the Robert W.Galvin Center for Electricity Innovation, Illinois Institute of Technology, Chicago, IL, USA, in 2019. He is currently with the School of Electrical and Electronic Engineering, North China Electric Power University, Beijing, China. His research interests include security and risk analysis for power systems with renewable energies, distributed optimization, and control of multiple sustainable energy sources in smart grids.

Liuyang Cai received the B.Eng. degree in electrical engineering and automation from China Three Gorges University, Yichang, China, in 2021. She is currently pursuing the M.Sc. degree in electrical engineering with North China Electric Power University, Beijing, China. Her areas of interest include demand response, smart grids, and renewable energy.

Mingze Tong received the B.Eng. degree in smart grid information engineering from North China Electric Power University, Beijing, China, in 2022. He is currently pursuing the M.Sc. degree in electrical engineering with North China Electric Power University, Beijing, China. His areas of interest include demand response, smart grids, and renewable energy.

Ting Wu received the B.Eng. degree in automation from Central South University, Changsha, China, in 2010, the M.Eng. degree in control theory and control engineering from Zhejiang University, Hangzhou, China, in 2013, and the Ph.D. degree from the Hong Kong Polytechnic University, Hong Kong, in 2017. She is currently an assistant professor with the School of Mechanical Engineering and Automation, Harbin Institute of Technology, Shenzhen, China. Her research interests include wide-area monitoring and control, integrated energy systems, electric vehicles, and cyber-physical power systems.

Peng Li received the Ph.D. degree in information management engineering from North China Electric Power University in 2014. After graduation, he joined the Economic and Technical Research Institute of State Grid Henan Electric Power Company as a senior economist. His research interests include rural energy Internet technology, energy transformation, distribution network planning and optimization.

Xiang Gao received the Ph.D. degree in electrical engineering from the Hong Kong Polytechnic University, Hong Kong, China, in 2021. She is now working at Shenzhen Polytechnic University, Shenzhen, China. Her research interests include electricity and carbon market, renewable energy resources, multi-agent reinforcement learning and stochastic optimization.

REFERENCES

[1] Y. Zhou, X. Fu, and H. Sun *et al*., "Prospects for energy internet of agricultural engineering in China," in *2019 IEEE 3rd Conference on Energy Internet and Energy System Integration (EI2)*, Changsha, China, Nov. 2019, pp.1807-1811.

[2] X. Fu and H. Niu, "Key technologies and applications of agricultural energy Internet for agricultural planting and fisheries industry," *Information Processing in Agriculture*, vol. 10, no. 3, pp. 416-437, Sept. 2023.

[3] A. Rejeb, K. Rejeb, and A. Abdollahi *et al*., "The interplay between the internet of things and agriculture: a bibliometric analysis and research agenda," *Internet of Things*, vol. 19, Aug. 2022.

[4] X. Chen, T. Yu, and Z. Pan *et al*., "Graph representation learning-based residential electricity behavior identification and energy management," *Protection and Control of Modern Power Systems*, vol. 8, no. 2, pp. 1-13, Apr. 2023.

[5] P. Wang, W. Wu, and B. Zhu *et al*., "Examining the impact factors of energy-related CO2 emissions using the STIRPAT model," *Applied Energy*, vol. 106, pp. 65-71, Jun. 2013.

[6] R. Morsali and R. Kowalczyk, "Demand response based day-ahead scheduling and battery sizing in microgrid management in rural areas," *IET Renewable Power*

Generation, vol. 12, no. 14, pp. 1651-1658, Oct. 2018.
[7] W. Huang, N. Zhang, and C. Kang *et al*., "From demand response to integrated demand response: review and prospect of research and application," *Protection and Control of Modern Power Systems*, vol. 4, no. 2, pp. 1-13, Apr. 2019.
[8] Z. Zheng, Q. Ai, and W. Xu *et al*., "A multi objective dispatch optimization strategy for economic operation of smart grids," *Power System Technology*, vol. 34, no. 2, pp. 7-13, Feb. 2010. (in Chinese)
[9] Y. Zhong, M. Huang, and C. Ye, "Multi-objective optimization of microgrid operation based on dynamic dispatch of battery energy storage system," *Electric Power Automation Equipment*, vol. 34, no. 6, pp. 114-121, Jun. 2014. (in Chinese)
[10] X. Zhang, M. Zhang, and W. Wang *et al*., "Scheduling optimization for rural micro energy grid multi-energy flow based on improved crossbreeding particle swarm algorithm," *Transactions of the Chinese Society of Agricultural Engineering*, vol. 33, no. 11, pp. 157-164, Jun. 2017. (in Chinese)
[11] X. Deng, "Research on optimal dispatching of active distribution network considering 'source-load-storage' collaborative interaction," M.S. thesis, the Department of Electrical and Electronic Engineering, North China Electric Power University, Beijing, China, 2019. (in Chinese).
[12] Y. Zhang, Y. Mu, and H. Jia *et al*., "Response capability evaluation model with multiple time scales for electric vehicle virtual power plant," *Automation of Electric Power Systems*, vol. 43, no. 12, pp. 94-103, Jun. 2019. (in Chinese).
[13] K. Xie, H. Hui, and Y. Ding, "Review of modeling and control strategy of thermostatically controlled loads for virtual energy storage system," *Protection and Control of Modern Power Systems*, vol. 4, no. 4, pp. 1-13, Oct. 2019.
[14] A. Aghajanzadeh and P. Therkelsen, "Agricultural demand response for decarbonizing the electricity grid," *Journal of Cleaner Production*, vol. 220, pp. 827-835, May 2019.
[15] A. S. Kocaman, E. Ozyoruk and S. Taneja *et al*., "A stochastic framework to evaluate the impact of agricultural load flexibility on the sizing of renewable energy systems," *Renewable Energy*, vol. 152, pp. 1067-1078, Jun. 2020.
[16] T. M. Khanna, "Using agricultural demand for reducing costs of renewable energy integration in India," *Energy*, vol. 254, Sept. 2022.
[17] X. Fu, Y. Zhou, and Z. Wei *et al*., (2023, April), "Optimal operation strategy for a rural microgrid considering greenhouse load control," *CSEE Journal of Power and Energy Systems*, pp. 1-11. Available: https://ieeexplore.ieee.org/document/10106208
[18] M. Wang, Z. Fan, and Y. Chen *et al*., "Quantification and application of cold load pick-up parameters based on temperature-controlled load variation characteristics," *Power System Protection and Control*, vol. 50, no. 21, pp. 54-64, Nov. 2022. (in Chinese)
[19] G. Aji, K. Hatou and T. Morimoto, "Modeling the dynamic response of plant growth to root zone temperature in hydroponic chili pepper plant using neural networks," *Agriculture*, vol. 10, no. 6, pp. 1-14, Jun. 2020.
[20] L. Wang and B. Wang, "Construction of greenhouse environment temperature adaptive model based on parameter identification," *Computers and Electronics in Agriculture,* vol. 174, no. 11, Jul. 2020.
[21] W. Wang, F. Liu, and J. Zheng *et al*., "Optimal regulation on micro energy grid based on time-shifting agricultural load," in *2017 IEEE Conference on Energy Internet and Energy System Integration (EI2)*, Beijing, China, Jan. 2018, pp.1-6.
[22] L. Zhang, P. Xu, and J. Mao *et al*., "A low cost seasonal solar soil heat storage system for greenhouse heating: Design and pilot study," *Applied Energy*, vol. 156, pp. 213-222, Oct. 2015.
[23] K. Wang, A. Pantaleo, and G. Mugnozza *et al*., "Technoeconomic assessment of solar combined heat and power systems based on hybrid PVT collectors in greenhouse applications," in *the 10th International Conference on Indoor Air Quality, Ventilation and Energy Conservation in Buildings,* Bari, Italy, Jun. 2019.
[24] D. Fan, S. Zhang, and H. Huang *et al*., "Three-stage day-ahead scheduling strategy for regional thermosta- tically controlled load aggregators," *Protection and Control of Modern Power Systems*, vol. 8, no. 2, pp. 1-11, Apr. 2023.
[25] H. Yang, R. Liang, and Y. Yuan *et al*., "Distributionally robust optimal dispatch in the power system with high penetration of wind power based on net load fluctuation data," *Applied Energy*, vol. 313, May 2022.
[26] R. M. Elavarasan, S. Leoponraj, and J. Vishnupriyan *et al*., "Multi-criteria decision analysis for user satisfaction induced demand side load management for an institutional building," *Renewable Energy*, vol. 170, pp. 1396-1426, Jun. 2021.
[27] M. M. Rahman, I. Khan, and D. L. Field *et al*., "Powering agriculture: present status, future potential, and challenges of renewable energy applications," *Renewable Energy*, vol. 188, pp. 731-749, Apr. 2022.
[28] J. Bai and X. Fu, "Review on electric energy substitution of agricultural energy internet in the context of carbon neutrality," *Integrated Intelligent Energy*, vol. 44, no. 6, pp. 1-11, Feb. 2022. (in Chinese)
[29] F. Lin, X. Cen, and M. Chen *et al*., "Application of microwave sulfur lamp filling technology in agricultural energy saving," *Power Demand Side Management*, vol. 20, no. 3, pp. 34-36, May 2018. (in Chinese).
[30] M. Fu, "Research on quick calculation of illuminance by unit capacity method," *Light & Lighting*, vol. 3, pp. 16-17, Jun. 2004. (in Chinese)
[31] K. Xu, X. Guo, and J. He *et al*., "A study on temperature spatial distribution of a greenhouse under solar load with considering crop transpiration and optical effects," *Energy Conversion and Management*, vol. 254, Feb. 2022.
[32] W. C. Yeh, C. Huang, and P. Lin *et al*., "Simplex simplified swarm optimisation for the efficient optimisation of parameter identification for solar cell models," *IET Renewable Power Generation*, vol. 12, no. 1, pp. 45-51, Jan. 2018.
[33] J. Du, P. Bansal, and B. Huang *et al*., "Simulation model of a greenhouse with a heat-pipe heating system," *Applied Energy*, vol. 93, pp. 268-276, May 2012.
[34] H. Ming, B. Xia, and K. Lee *et al*., "Prediction and assessment of demand response potential with coupon incentives in highly renewable power systems," *Protection and Control of Modern Power Systems*, vol. 5, no. 2, pp. 1-14, Apr. 2020.
[35] P. J. C. Vogler-Finck, P. Bacher, and H. Madsen, "Online short-term forecast of greenhouse heat load using a weather forecast service," *Applied Energy*, vol. 205, pp. 1298-1310, Nov. 2017.